FEBS Letters 580 (2006) 5411–5422

STD and TRNOESY NMR studies for the epitope mapping of the phosphorylation motif of the oncogenic protein β-catenin recognized by a selective monoclonal antibody

Simon Megy[a], Gildas Bertho[a], Josyane Gharbi-Benarous[a], Françoise Baleux[c], Richard Benarous[b], Jean-Pierre Girault[a,*]

[a] *Université Paris V-René Descartes, Laboratoire de Chimie et Biochimie Pharmacologiques et Toxicologiques (UMR 8601 CNRS), 45 Rue des Saint-Pères, 75270 Paris Cedex 06, France*

[b] *Université Paris V-René Descartes, U567-INSERM, UMR 8104 CNRS, Institut Cochin-Département des Maladies Infectieuses, Hôpital Cochin Bat. G. Roussy, 27 Rue du Faubourg St-Jacques, 75014 Paris, France*

[c] *Unité de Chimie Organique, URA CNRS 487, Institut Pasteur, 28 Rue du Dr Roux, 75724 Paris Cedex, France*

Received 27 February 2006; revised 30 June 2006; accepted 9 August 2006

Available online 14 September 2006

Edited by Christian Griesinger

Abstract The interaction of the P-β-Cat$^{19–44}$ peptide, a 26 amino acid peptide (K^{19}AAVSHWQQQSYLDpSGIHpSGATTTAP^{44}) that mimics the phosphorylated β-Catenin antigen, has been studied with its monoclonal antibody BC-22, by transferred nuclear Overhauser effect NMR spectroscopy (TRNOESY) and saturation transfer difference NMR (STD NMR) spectroscopy. This antibody is specific to diphosphorylated β-Catenin and does not react with the non-phosphorylated protein. Phosphorylation of β-Catenin at sites Ser33 and Ser37 on the DSGXXS motif is required for the interaction of β-Catenin with the ubiquitin ligase SCF$^{β\text{-TrCP}}$. β-TrCP is involved in the ubiquitination and proteasome targeting of the oncogenic protein β-Catenin, the accumulation of which has been implicated in various human cancers. The three-dimensional structure of the P-β-Cat$^{19–44}$ in the bound conformation was determined by TRNOESY NMR experiments; the peptide adopts a compact structure in the presence of mAb with formation of turns around Trp25 and Gln26, with a tight bend created by the DpS^{33}GIHpS^{37} motif; the peptide residues (D32-pS37) forming this bend are recognized by the antibody as demonstrated by STD NMR experiments. STD NMR studies provide evidence for the existence of a conformational epitope containing tandem repeats of phosphoserine motifs. The peptide's epitope is predominantly located in the large bend and in the N-terminal segment, implicating bidentate association. These findings are in excellent agreement with a recently published NMR structure required for the interaction of β-Catenin with the SCF$^{β\text{-TrCP}}$ protein.

Keywords: β-Catenin oncogenic protein; P-β-Catenin phosphorylated peptide; Epitope mapping; Antibody; P-β-Catenin/antibody complex; STD NMR; TRNOESY; Restrained molecular dynamics; Bound structure; Binding fragment

1. Introduction

β-Catenin (β-Cat) is an oncogenic protein that plays an important role in the Wnt signaling pathway [1,2] and is an important component of the cadherin cell-adhesion complex (Fig. 1). Wnt genes encode secreted signaling molecules that play important roles in development and tumorigenesis [3,4]. Deregulation of Wnt signaling is responsible for several human malignancies [5,6]. It is well known that serine-phosphorylation of β-Catenin by the Axin-glycogen synthase kinase (GSK)-3β complex targets β-Catenin for degradation by the ubiquitination–proteosome pathway [7–10], and mutations at critical phosphoserine residues stabilize β-Catenin and cause human cancers [11–13]. β-Catenin phosphorylation results in its degradation when phosphorylated β-Catenin is specifically recognized by β-transducin repeat-containing protein (β-TrCP), an F-box/WD40-repeat protein that also associates with Skp1, an essential component of the ubiquitination apparatus [14].

It has been demonstrated that β-Catenin binds to the F-box WD40 protein β-TrCP [15,16], the receptor component of the multi subunit Skp1-Cullin-FBox (SCF)$^{β\text{-TrCP}}$E3 ubiquitin ligase complex through its phosphorylated serine residues at positions 33 and 37 [17]. β-TrCP is also involved in the ubiquitination and proteasome targeting of: (i) the HIV-1 protein Vpu [17], which enhances the release of new virus particles from the plasma membrane of cells infected with HIV-1 [18] whereas it induces the degradation of the CD4 receptor in the endoplasmic reticulum; (ii) IκBα, the inhibitor of master transcription factor NF-κB [16,19,20]; and (iii) ATF4, a member of the family of transcription factors [21]. The antigenic peptides containing the **DpSGXXpS** motif constitute β-TrCP-associated epitopes. The SCF$^{β\text{-TrCP}}$ complex specifically recognizes a 22-residue β-Catenin polypeptide, a HIV-1 encoded virus protein U (Vpu) peptide fragment of 22 amino acids, and a 19-amino acid motif in IκBα in a phosphorylation-dependent manner

*Corresponding author. Fax: +33 1 42 86 83 87.
E-mail address: Jean-Pierre.Girault@univ-paris5.fr (J.-P. Girault).

Abbreviations: ARIA, ambiguous restraints for iterative assignment; mAb, monoclonal antibody; β-Cat, β-Catenin protein; P-β-Cat, phosphorylated β-Catenin; β-TrCP, β-transducin repeat containing protein; SCF, Skp1-Cullin-FBox; NOESY, nuclear Overhauser effect spectroscopy; Vpu, HIV-1 encoded virus protein U; rmsd, root-mean-square deviation; STD, saturation transfer difference; TRNOESY, transferred nuclear Overhauser effect spectroscopy; TOCSY, total correlation spectroscopy

0014-5793/$32.00
doi:10.1016/j.febslet.2006.08.084

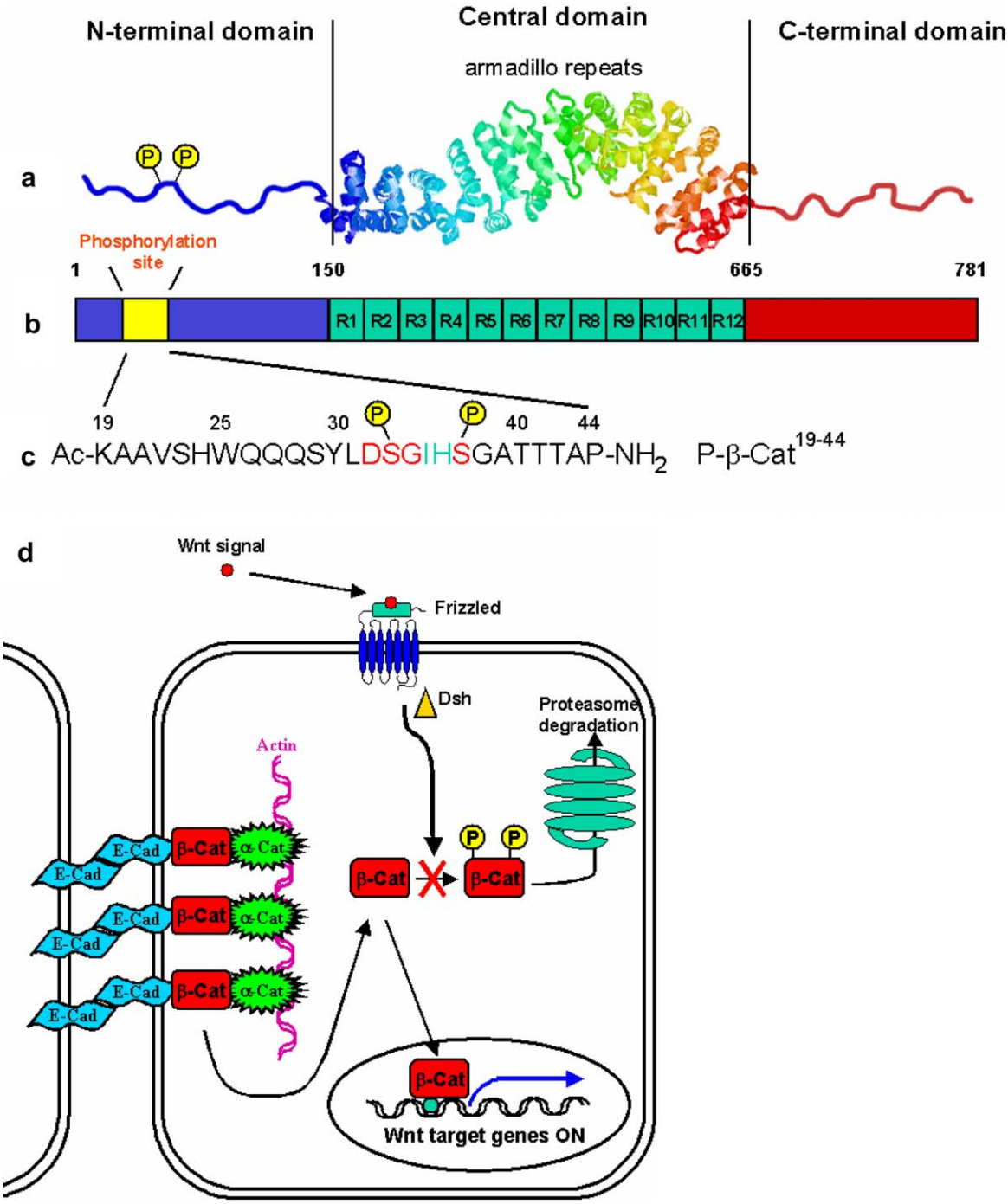

Fig. 1. (A) Schematic representation of the β-Catenin. (a) The three-dimensional structure of a protease-resistant fragment of β-Catenin containing the armadillo repeat region. The core region of β-Catenin is composed of 12 copies of a 42 amino acid sequence motif known as an armadillo repeat. The 12 repeats form a super helix of helices that features a long, positively charged groove of the proteolyse resistant fragment [52]. The structure of the N and C terminal domains remain unresolved. (b) Primary structure sequence of the full β-Catenin protein. The 12 armadillo repeats are shown in green. The phosphorylation site containing the consensus motif DpSGXXpS is shown in yellow. (c) The sequence of the phosphorylated β-Catenin fragment, P-β-Cat$^{19-44}$ which was investigated in the present work. (d) The α-cadherin/β-Catenin complex connects to the actin via α-Catenin and some actin-binding proteins, forming a rigid cytoskeleton. β-Catenin is involved in the Wingless/Wnt signaling pathway. When cells are exposed to Wnt signal, cell surface receptors are activated and block β-Catenin phosphorylation and its subsequent ubiquitination. β-Catenin is thus diverted from the proteasome, and it accumulates and enters the nucleus, where it finds a partner of the TCF/LEF family. Together, they activate new gene expression programs.

[16]. The signal for the recognition of all these cellular ligands by β-TrCP is the phosphorylation of the serine residues present in a conserved motif, D**pS**GXX**pS** for β-Catenin, Vpu, IκBα and D**pS**GXXX**pS** for ATF4. It was recently shown that Vpu is a competitive inhibitor of β-TrCP that impairs the degradation of SCF$^{\beta\text{-TrCP}}$ substrates as long as Vpu has an intact D**pS**GXX**pS** phosphorylation motif and can bind to β-TrCP [22].

Antibodies which recognize epitopes implicated in various human cancers have been developed [23]. A monoclonal antibody reacting specifically with β-Catenin phosphorylated at serine Ser33 and Ser37 is an essential tool in defining the interactions, distribution, and regulation/deregulation of β-Catenin and its role in signal transduction. A specific monoclonal antibody (mAb) was generated against the P-β-Cat$^{32–45}$ peptide (Fig. 1), D**pS**GIH**pS**GATTTAPS (numbers refer to the β-Catenin protein). We postulate that structural similarities can occur between the small peptide ligand and the same sequence found within the intact protein, so when anti-ligand monoclonal antibodies recognizing the peptide were obtained, they are very good tools for the evaluation of structural elements of the intact protein bound by the natural receptor (β-TrCP). This antibody is specific to the native phosphorylated β-Catenin containing the D**pS**^{33}GIH**pS**^{37} amino acid sequence in the central part, and does not react with the nonphosphorylated protein. In addition, we showed previously that the P-β-Cat$^{19–44}$ phosphorylated peptide has structural features different from those of its parent β-Cat$^{19–44}$ peptide [24].

Antibody recognizes the P-β-Cat$^{32–45}$ peptide, a small antigen-binding fragment, and a fragment generally retains the specificity and affinity of the entire parent protein. Antireceptor antibodies have been successfully used for the investigation of ligand–receptor interactions as the internal complementary binding region of the receptor binding site [25,26]. This latter approach can be especially useful when (a) isolation of the receptor in a suitable form for structural studies of the receptor–ligand interaction is extremely difficult or (b) little information is available for its active state [27]. Thus, determination of the conformational features of the P-β-Catenin D**pS**GXX**pS** moiety implicated in antibody binding should provide complementary information about the structural parameters characterizing β-Catenin-β-TrCP receptor interaction [28] to improve the understanding of the substrate specificity of SCF$^{\beta\text{-TrCP}}$. The structural characterization of the D**pS**GXX**pS** moiety may have an additional interest. This will contribute to the design of molecules mimicking the structure of the β-Catenin adhesion site and possibly thus acting as a potent model for the D**pS**GXX**pS**-protein complex.

Here, we present the STD NMR epitope mapping and TRNOE-based conformational analysis of the P-β-Cat$^{19–44}$ peptide bound to the monoclonal antibody, mAb. The transferred nuclear Overhauser effect spectroscopy (TRNOESY) experiment has been used to determine the conformations of a wide range of small ligands in the protein-bound state by focusing on the easily detected NMR signals of the free ligands [29]. The mAb-bound P-β-Cat$^{19–44}$ peptide conformation was finally elucidated by molecular dynamics simulation, an approach combining dynamical annealing and refinement protocols. Saturation transfer difference (STD) NMR [30–32] is a technique that can be used to characterize and identify binding. It can also be used to identify the binding epitope of ligands to a protein receptor [32].

2. Results

2.1. Binding of mAb BC-22 to the phosphorylated P-β-Cat$^{19–44}$ peptide

The monoclonal anti-diphospho-β-Catenin (**pSer33** and **pSer37**) reacts specifically with β-Catenin diphosphorylated

Table 1
^{1}H NMR chemical shifts (ppm) of the free P-β-Cat$^{19–44}$ peptide from TSP-d_4[a]

Residue	δ NH	δ H_α	δ H_β	δ H_γ	δ H_δ	δ others
Ac						2.03
Lys 19	8.42	4.24	1.79	1.45	1.78	2.99
Ala 20	8.53	4.28	1.38			
Ala 21	8.47	4.31	1.45			
Val 22	8.27	4.12	2.04	0.91/0.88		
Ser 23	8.52	4.42	3.78/3.73			
His 24	8.59	4.63	3.08	2H 8.11; 4H 7.01		
Trp 25	8.16	4.56	3.25	NεH 10.25		
				2H 7.23; 4H 7.53; 5H 7.14; 6H 7.25; 7H 7.49		
Gln 26	8.14	4.11	1.94/1.78	2.10		6.92/7.51
Gln 27	8.26	4.12	2.04/1.98	2.34		7.00/7.65
Gln 28	8.53	4.28	2.01/1.96	2.31		6.95/7.59
Ser 29	8.44	4.42	3.79			
Tyr 30	8.30	4.56	2.96/3.03		7.08	6.79
Leu 31	8.21	4.32	1.53	1.45	0.83/0.88	
Asp 32	8.21	4.61	2.75			
pSer 33	9.22	4.46	4.18/4.12			
Gly 34	8.62	3.92				
Ile 35	8.07	4.03	1.79	$H_{\gamma1}$ 1.15/1.44		
$H_{\gamma2}$ 0.82	0.82					
His 36	8.80	4.81	3.15/3.32	2H 8.46; 4H 7.23		
pSer 37	9.37	4.47	4.11			
Gly 38	8.78	4.01				
Ala 39	8.28	4.42	1.44			
Thr 40	8.45	4.45	4.27	1.22		
Thr 41	8.38	4.46	4.26	1.22		
Thr 42	8.35	4.33	4.17	1.22		
Ala 43	8.57	4.61	1.38			
Pro 44	–	4.39	2.32/1.96	2.05	3.67/3.81	
NH_2						7.79/7.14

[a]Spectra were recorded at 278 K and pH 7.2 in 20 mM sodium phosphate buffer and a 9:1 $H_2O/^2H_2O$ mixture (by volume).

at Ser33, and Ser37. The mAb was tested in a direct ELISA for binding to block the P-β-Cat$^{19–44}$ peptide, which contained the consensus sequence D**pS**GXX**pS**. At the peptide level, the antibody recognizes efficiently the P-β-Cat$^{19–44}$ peptide and not the nonphosphorylated one [23]. Given the uncertainties in the effective concentration of mAb that was immobilized on the ELISA plate, the K_D for peptide P-β-Cat$^{19–44}$ bound to mAb was estimated to be between 100 and 500 μM. This range of binding affinity made the peptide likely to be suitable for TRNOESY NMR experiments, which require fast exchange between the free and bound states.

2.2. NMR resonance assignments

^{1}H chemical shifts and resonance assignments were established using two-dimensional ^{1}H-^{1}H TOCSY (total correlation spectroscopy) and nuclear Overhauser effect spectroscopy (NOESY) experiments [33] and are reported in Tables 1 and 2. Interestingly, in the presence of antibody, a slight low-frequency (shielded) shift of the amide protons was observed for residues His24 and Trp25; however, observation of an opposite shift, high-frequency (unshielded) shifted HN resonance particularly for Asp32, pSer33, Gly34 and pSer37 may be an indicator of intermolecular contact of the phosphorylated motif with the binding site. The unshielding effect observed for the negatively charged fragment D32-T42 could reflect the positive charged contact of the antibody surface. Hence the binding region encompasses the immunogene diphosphorylated peptide 32–45 region. A low shielding effect in the upstream hydrophobic region could also indicate an additional contribution in the interaction of P-β-Cat$^{19–44}$ peptide with mAb BC-22.

2.3. Interaction of P-β-Cat$^{19–44}$ with mAb BC-22

The dissociation constant was estimated from the line broadening at different peptide:antibody ratios to be ~200 μM [29]. These measurements show that the phosphorylated D**pS**GIH**pS** motif is necessary for binding, but residues from the longer peptide P-β-Cat$^{19–44}$ do contribute additional binding energy. Because of the low mAb:peptide molar ratio, free and bound peptide molecules were in rapid chemical exchange and only a single set of broadened ligand resonances was observed. To provide additional information regarding the peptide mode of binding, STD NMR experiments (Fig. 2) were performed [30–32]. The STD NMR technique is a method which could give an epitope mapping by NMR spectroscopy. Resonances of the protein are selectively saturated, and in a binding ligand, enhancements are observed in the difference (STD NMR) spectrum resulting from subtraction of this spectrum from a reference spectrum in which the protein is not saturated (Fig. 2) [30–32]. Protons of the ligand which are in close contact with the protein can be identified from the STD NMR spectrum, because they are expected to be saturated to the highest degree. The individual signal protons of the P-β-Cat$^{19–44}$ peptide are best analyzed from the intensity values than the integral values in the reference (I_0) and STD spectra ($I_{STD} = I_0 - I_{sat}$). The spectral region corresponding to the amino protons is well resolved and can be used to classify the amino acid residues relevant for interaction with the antibody. The moderate degree of overlapping for the amide protons allowed us to calculate the intensity for all the visible amide protons of the peptide. The signals observed in the 1D spectra for the amide protons of the whole peptide are summarized in Fig. 2.

Table 2
^{1}H NMR chemical shifts (ppm) of the P-β-Cat$^{19–44}$ peptide bound to antibody mAb from TSP-d_4[a]

Residue	δ NH	δ $H_α$	δ $H_β$	δ $H_γ$	δ $H_δ$	δ others
Ac						2.03
Lys 19	8.42	4.25	1.81	1.46	1.71	3.00
Ala 20	8.52	4.29	1.39			
Ala 21	8.46	4.32	1.39			
Val 22	8.27	4.12	2.05	0.93/0.89		
Ser 23	8.52	4.42	3.80/3.74			
His 24	8.58	4.63	3.09	2H 8.16; 4H 7.10		
Trp 25	8.15	4.57	3.25	NεH 10.24 2H 7.24; 4H 7.54; 5H 7.15; 6H 7.25; 7H 7.49		
Gln 26	8.14	4.11	1.96/1.79	2.11		6.93/7.51
Gln 27	8.26	4.12	2.05/1.99	2.35		7.01/7.66
Gln 28	8.53	4.29	2.01/1.96	2.31		6.96/7.60
Ser 29	8.44	4.42	3.80			
Tyr 30	8.30	4.57	2.96/3.04		7.09	6.81
Leu 31	8.21	4.32	1.55	1.45	0.83/0.89	
Asp 32	8.22	4.61	2.75			
pSer 33	9.26	4.45	4.18/4.12			
Gly 34	8.63	3.93				
Ile 35	8.07	4.04	1.80	$H_{γ1}$ 1.19/1.44 $H_{γ2}$ 0.82	0.82	
His 36	8.79	4.81	3.16/3.32	2H 8.10; 4H 7.23		
pSer 37	9.40	4.46	4.10			
Gly 38	8.77	4.02				
Ala 39	8.29	4.42	1.45			
Thr 40	8.45	4.45	4.27	1.24		
Thr 41	8.39	4.46	4.26	1.22		
Thr 42	8.36	4.33	4.17	1.23		
Ala 43	8.57	4.61	1.38			
Pro 44		4.39	2.32/1.96	2.07/2.03	3.68/3.82	
NH_2						7.79/7.15

[a]Spectra were recorded at 278 K and pH 7.2 with a 100:1 P-β-Cat:mAb ratio, and 20 mM sodium phosphate buffer in a 9:1 $H_2O/^2H_2O$ mixture (by volume).

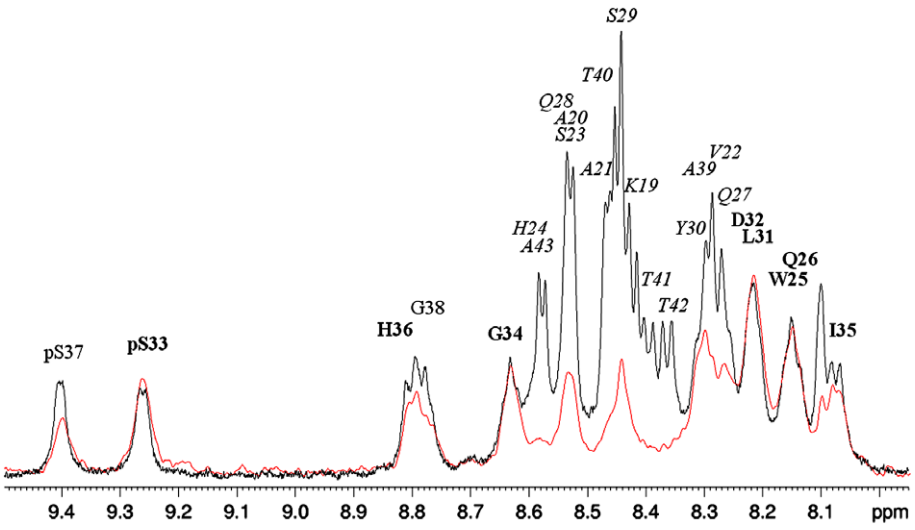

Fig. 2. Epitope mapping of the P-β-Cat$^{19–44}$ peptide in the presence of mAb, for a peptide:antibody ratio of 100:1. Expansion of the region containing resonances of the amide protons: Reference 1D ^{1}H spectrum (in black) of the P-β-Cat$^{19–44}$ peptide in association with the mAb antibody and 1D ^{1}H STD NMR spectrum (in red) of the P-β-Cat$^{19–44}$ peptide in association with the mAb antibody, showing enhancements of resonances of protons making close contacts with the antibody-combining site. STD values are obtained after peak picking intensities compared to the 1D with the exact values of chemical shifts of the HN (in bold: amino acids with intense relative STD, and in italic: amino acids with weak relative STD). Variations of the chemical shifts between the HN are equal to or higher than 0.01 ppm. There are only Ala20 and Ser23, which pose problem since they leave together to 8.52 ppm. The value given can thus correspond only to the average of relative STD value found for each one.

The signal obtained with the largest I_{STD}/I_0 value, the pSer33 and Asp32 H–N proton, was normalized to 100% (Fig. 3). The relative degree of saturation for the individual protons, normalized to that of pSer33 or Asp32, can be used to compare the STD effect [32]. For reference, the STD NMR spectrum was recorded with a sample containing the nonphosphorylated β-Cat$^{19–44}$ peptide, and all signals from nonbinding peptide were completely eliminated.

Fig. 2 shows the 1D STD NMR spectrum and a normal ^{1}H-spectrum of the complex of P-β-Cat$^{19–44}$ with the antibody. The pSer33 (99%) and Asp32 (100%) H–N resonances, and other **pS**GIH**pS** motif resonances belonging to either Gly34 (85%), Ile35 (74%), His36 (61%) or pSer37 (52%), have similar STD intensities between 50% and 100% (Fig. 4). Obviously, these residues have more and tighter contacts with the antibody's surface. On the other hand, side chains resonances and H-N resonances of Trp25 (79%), Gln26 (70%) and

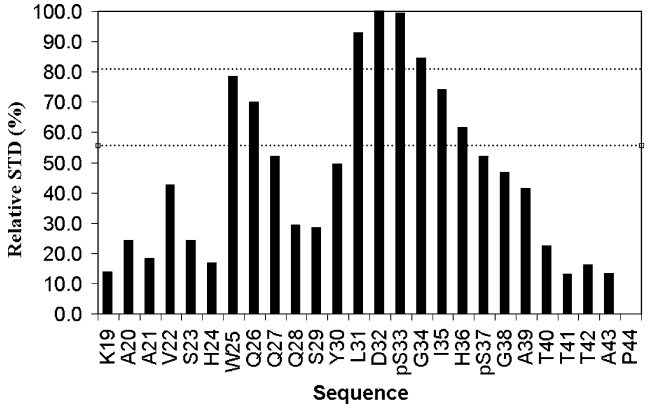

Fig. 3. Relative STD intensities (in percent) of the amide protons of the individual amino acids calculated for each amino acid of the P-β-Cat$^{19–44}$ peptide from the 1D spectrum.

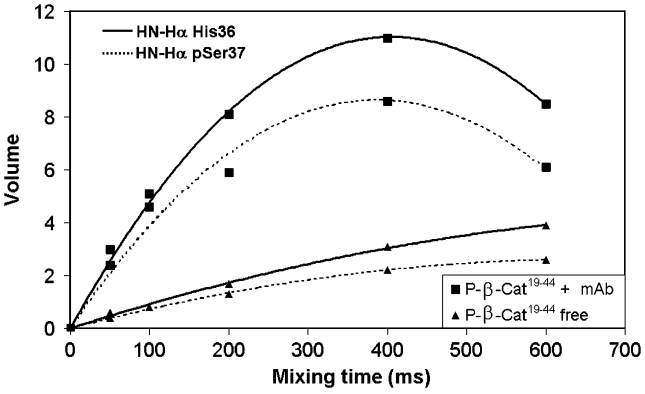

Fig. 4. TRNOE build-up rates of P-β-Cat$^{19–44}$ peptide with or without mAb vs. mixing time (ms). The ligand to antibody ratio is 100:1. The curves represent the intra-residue connectivity HN/Hα of His36 and **pSer37**.

Gln27 (52%) have similar larger STD intensities, ranging from 50% to 80%, indicating that these side chains are involved in the epitope. The lowest intensities are found for the protons of the N-terminal group, residues K19-A21 and the C-terminal group, residues T40-A43, which reach values of only 10–20%. Proton signals of the acetyl group at 2.03 ppm and of the amide group at 7.79 ppm and 7.15 ppm strongly decreased or disappeared completely in the STD spectra indicating that the terminal group are not involved in the interaction. Thus, a clear distinction between protons with a strong contact to the protein and the others can be made.

The combination of STD NMR epitope mapping data with knowledge of the bound conformation of the ligand, which may be obtained by TRNOESY experiments, is a powerful method for building up models of antibody–ligand interaction [34,35].

2.4. Conformation of the antibody-bound phosphorylated P-β-Cat$^{19-44}$ peptide

The bound conformation of the peptide was investigated by TRNOESY experiments [36]. According to the TRNOE build-up curves [37] of P-β-Cat$^{19-44}$ peptide, the mixing time of the transferred NOE experiment was set to 200 ms. The observation of TRNOE cross-peaks, when mAb was added, attested to peptide-antibody interaction and the restricted flexibility of the mAb-bound peptide. We observed faster rate of build up for the peptide in presence of mAb (Fig. 4), which indicated the binding of the peptide to the mAb. The observation of supplementary TRNOE cross-peaks (Fig. 5), when the antibody was added, attested the peptide–protein interaction. Significant differences were observed between the NOESY spectra of the free peptide and the one of the petide bound to the antibody, indicating that the cross-peaks observed in presence of antibody are in fact TRNOEs (Figure S1 in Supporting Information). For instance, there is 12 new $d_{\alpha N}(i, i+2)$ observable connectivities (between residues 19–21, 20–22, 21–23, 23–25, 24–26, 26–28, 27–29, 28–30, 35–37, 37–39, 39–41 and 40–42) for the bound peptide. In a similar manner, four $d_{\alpha N}(i, i+3)$ appeared in the N-terminal part of the bound peptide (21–24, 22–25, 25–28 and 26–29), and two $d_{\alpha\beta}(i, i+3)$ were newly present on each side of the D**pS**^{33}GIH**pS**^{37} motif (30–33 and 37–40). The $d_{\alpha N}(i, i+4)$ are also numerous only in the bound peptide and essentially in the N-terminal part (19–23, 21–25, 23–27, 24–28, 25–29, 26–30, 27–31 and 35–39, 39–43).

A summary of sequential $d(i, i+1)$ and medium-range $d(i, i+2)$ and $d(i, i+3)$ ^{1}H–^{1}H NOE connectivities is presented in Fig. 5. The large number of TRNOESY connectivities involving side chain protons of the aromatic residues (His24, Trp25, Tyr30, and His36) as well as the side chain protons of many residues and the main backbone appeared upon addition of the antibody (for instance, between 2H of Trp25 and 2H of His24, or between 2H of His36 and Hα of Gly38) suggests that the aromatic side chains rings are rather frozen in the bound state.

The TRNOE spectrum exhibits a great number of NOEs, including intense and medium NN(i, $i+1$) connectivities (Fig. 5), suggesting secondary structures (helix, turn, bend, or strand). The αN(i, $i+2$), αN(D32-G34, pS33-I35, I35-pS37) peaks argue in favor of a folded structure for the D**pS**^{33}GIH**pS**^{37} sequence which includes the pSer phosphorylated site. In this motif, where a bend was apparent, the four αN(i, $i+2$) and the two αβ(i, $i+3$) αβ(Y30-pS33 and H36-A39) connectivities helped to define this bend. The αN(i, $i+3$), and αβ(i, $i+3$) connectivities attests that the phosphorylated peptide adopts a well-defined and folded structure in the presence of the antibody. In particular, residues 20–32 have NOE connectivities that suggest the presence of a turn or half-turn structure. The seven αN(i, $i+3$) connectivities are diagnostic of a propensity for a turn region located just before the D**pS**^{33}GIH**pS**^{37}G motif.

To study the conformation of the bound state of P-β-Cat$^{19-44}$ in the presence of the mAb antibody the distance restraints were incorporated into a simulated annealing protocol using ambiguous restraints for iterative assignment (ARIA) [38,39]. A set of 20 structures produced by simulated annealing was subjected to energy minimization, followed by checks for correct geometry and agreement with the distance restraints (Fig. 6). The structural models fit the NMR data well, with no violations of experimental distance restraints greater than 0.3–0.5 Å. The positions of the backbone and most side chain atoms were well defined by the NMR restraints. Structural statistics are presented in Table 3.

The average root-mean-square difference for superimposition of the 10 structures with the lowest NOE restraint energy was 2.1 Å for the backbone atoms (N, C_α, C, and O) of residues 19–37. Lower root-mean-square deviation (rmsd) was obtained when the superposition was carried out separately for the central segment 25–36 (1.4 Å) and the partially-helical region at the N-terminal segment 19–25 (1.5 Å). This is con-

Fig. 5. Sequential $d(i, i+1)$, and medium range $d(i, i+2)$, and $d(i, i+3)$ ^{1}H-^{1}H TRNOE connectivities in the P-β-Cat$^{19-44}$ peptide (sequence at the top) in the presence of the mAb antibody at 278 K and pH 7.2. The thickness of the lines reflects the relative intensities of the NOEs within the individual plots.

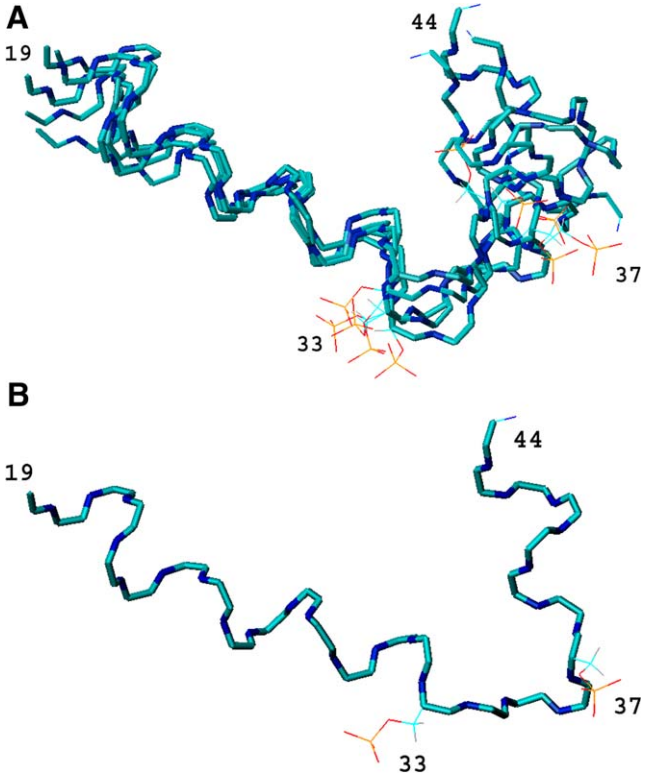

Fig. 6. NMR TRNOE-derived structures of the bound peptide P-β-Cat$^{19-44}$ peptide in the presence of the mAb antibody. (A) Twenty structures of P-β-Cat$^{19-44}$ were generated after eight iterations with ARIA software. The best five are displayed. The molecules are fitted from residue 25 to residue 36. (B) The minimum energy-minimized conformer with the best fit of proton distance constraints.

Table 3
Structural statistics of the final 10 NMR structures of P-β-Cat$^{19–44}$ bound to the mAb antibody

No. of experimental distance restraints	
Unambiguous NOE	311
Ambiguous NOE	92
Total NOEs	403[a]
No. of experimental broad dihedral restraints	23
NOE violations >0.3 Å per structure	1.5
Rms differences from mean structure[b] (Å)	
Backbone (residues 19–25)	1.5 ± 0.4
Heavy (residues 19–25)	2.6 ± 0.6
Backbone (residues 25–36)	1.4 ± 0.4
Heavy (residues 25–36)	2.8 ± 0.6
Ramachandran plot of residues[c] (%)	
In most favored regions	57.7
In additional allowed regions	39.6
In generously allowed regions	2.3
In disallowed regions	0.4

[a]NOEs: 194 intra-residue, 98 sequential, 98 medium-range and 13 long-range.
[b]Calculated with MOLMOL.
[c]Calculated with PROCHECK NMR.

firmed by the local rmsd (calculated on three residues) for each residue of the bound structure of P-β-Cat$^{19–44}$. The increased or decreased flexibility of the segments may be appreciated from the magnitude of the local rmsd which highlights a higher stability of residues 20–31 (local rmsd values around 0.1 Å). The values are slightly higher for residues D32-pS33 (in the range of 0.4–0.5 Å), and drop significantly until 0.7–0.8 Å for residues G34-H36 and T41-A43. There is more disorder in the terminal parts of the peptide, which are less well defined by the TRNOEs. This is consistent with the total number of NOE constraints observed per residue. Interestingly, the well-ordered part of the peptide corresponds to the residues 22–37, which were the most involved in the binding with the antibody, a hypothesis consistent with the STD NMR data.

3. Discussion

3.1. Conformation of P-β-Cat$^{19–44}$ Bound to mAb

The ensemble of five lowest energy structures is shown in Fig. 6A. The structures are fitted from residues 25 to 36. The bound conformation of the peptide showed a propensity for turn formation in N-terminal residues, and a bend including the D**pS**^{33}GIH**pS**^{37}G phosphorylation motif (Fig. 6B). When bound to the mAb, the phosphorylated peptide adopts a folded structure, which reflects the local rearrangement of the D**pS**GXX**pS** phosphorylation site at the interface with the mAb. The conformation of the mAb-bound P-β-Cat$^{19–44}$ peptide is significantly represented in the free phosphorylated peptide (Fig. 7). Interestingly, the main structural changes are observed in the motif region of the P-β-Cat$^{19–44}$ peptide, which is modified upon binding as reflected by a different orientation of the phosphorylated residue **pSer37**. Hence, in the free P-β-Cat$^{17–48}$ peptide structure, the phosphate groups have a nearly coplanar orientation while in the bound structure they have an opposite coplanar orientation (Fig. 7B).

The bend is similarly found in the mAb and also in the β-TrCP-bound P-β-Cat$^{17–48}$ peptide [28], as shown in Fig. 8.

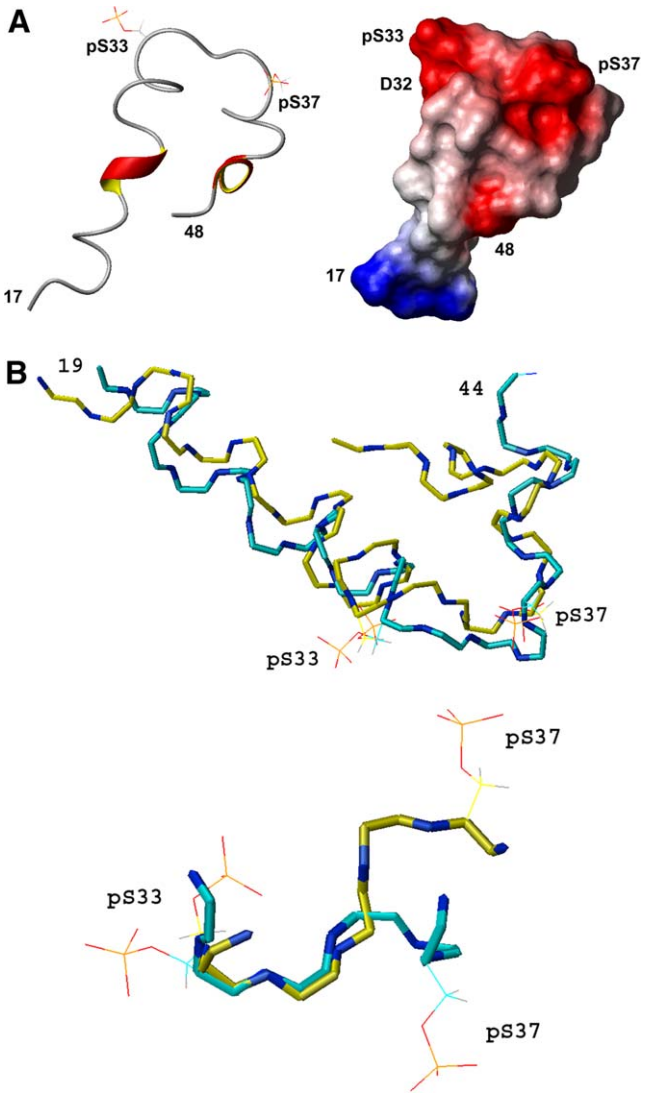

Fig. 7. (A) The minimum energy conformer of the free P-β-Cat$^{17–48}$ which contains phosphoserines **pSer33** and **pSer37**. The surface representation is colored according to the electrostatic potential (red for the negative region and blue for the positive surface). (B) Superimposition of the mAb P-β-Cat$^{19–44}$ bound peptide (in blue), and the P-β-Cat$^{17–48}$ free peptide (in yellow) and superimposition of the ^{32}D**pS**GXX**pS**^{37} fragment.

To elucidate the basis of β-TrCP recognition, the structure of the P-β-Cat$^{17–48}$ peptide bound to the F-Box Protein β-TrCP was previously determined by NMR and molecular dynamics [28]; the residues 30–37 formed a bend while the phosphate groups point away. The β-turn motif also plays a central role in the crystal structure of the human β-TrCP1-Skp1 complex bound to a fragment β-catenin peptide [40] (Fig. 9A and B). In the crystal structure, only an 11 residue segment (residues 30–40) of the β-Catenin, centered on the doubly phosphorylated motif (D**pS**^{33}GXX**pS**^{37}), makes the largest number of contacts with β-TrCP1 (Fig. 9B). The phosphoserine, aspartic acid, and hydrophobic residues of the motif makes direct contacts with β-TrCP1. Interaction of β-Catenin with the P-β-Cat specific monoclonal antibody relies on the D**pS**GXX**pS** motif, similar to that found in the other substrates of β-TrCP (IκBα and HIV-1 Vpu). The turn conformation is often important in allowing peptide side

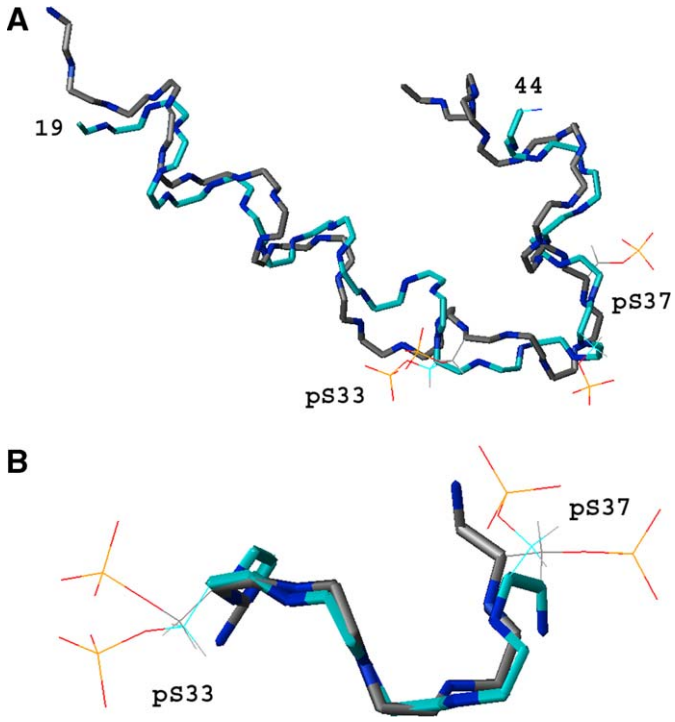

Fig. 8. (A) Superimposition of the mAb-P-β-Cat$^{19–44}$ bound peptide (in blue), and the β-TrCP-P-β-Cat$^{17–48}$ bound peptide (in grey) [28]. The two structures are fitted from residue 33 to 36. (B) Superimposition of the ^{32}**DpSGXXpS**^{37} fragment of the mAb P-β-Cat$^{19–44}$ bound peptide (in blue), and the β-TrCP-P-β-Cat$^{17–48}$ bound peptide (in grey) [28].

chains to be positioned correctly within the binding site and to make specific contacts with residues within the site. This is clearly important here as is shown by the epitope mapping data where (H24-W25) and (D32-S37) side chains contact the site.

3.2. The epitope mapping of the bound P-β-Cat$^{19–44}$ with mAb

The STD amplification factors of the amide protons were classified (Fig. 3). Nearly all the NH of the **DpSGXXpS** motif interact strongly with the corresponding amino acids inside the paratope. In the bound structures of P-β-Cat$^{19–44}$ peptide, the **DpSGXXpS** motif and N-terminal part are well-defined regions characterized by a low local rmsd and these regions are involved in the binding surface contact of β-Catenin with the mAb protein.

The **DpS**^{33}GXX**pS**^{37} bend form a negatively charged surface (in red, Fig. 7A) that would provide a plausible binding region similar to the negative β-Catenin substrate peptide in contact with the positive protein β-TrCP surface shown in Fig. 9A. The position of **DpSGXXpS** within a larger, extended epitope may be designed to present the phosphate group to antibodies. The phosphate group of **pSer33** is able to make the largest number of contacts making electrostatic interactions and hydrogen bonds. Asp32, which is an invariant binding motif residue, is also able to make an extensive contact as its side chain allows hydrogen bonding with some residues of mAb BC-22. Gly34, also an invariant binding motif residue, is able to pack with the antibody receptor in an environment with little space for a nonglycine residue.

Hence, we made the superimposition from residue 33 to 36 of the lowest energy structure of the bound peptides with mAb and β-TrCP (Fig. 8B), and the recent crystal structure (Fig. 9C). A good agreement is found between the three structures, essentially for the **DpSGX** region of the consensus **DpSGXXpS** motif. The side chain of the first phosphoserine **pSer33** points in the same direction and the phosphate groups are found close together. However, in the consensus **DpSGXXpS** motif, the **XpS** region containing the second phosphoserine is found to be very different which involved a large distance between the phosphate groups of **pSer37** in the three structures. Interestingly, this result highlighted the strong implication that the first phosphoserine **pSer33** of β-catenin should have with mAb and β-TrCP (Figs. 9B and C), while the phosphate group of **pSer37** could interact with many positively charged amino acids. Thus, the main difference observed between all the known bound structures of peptides interacting with mAb or β-TrCP resides in different positions of the phosphorylated residue **pSer37** (Figs. 9B and C). An excellent agreement is found between the amide protons with the strongest relative STD intensities and the corresponding residues in the crystal structure. Thus, either by using STD NMR experiments or by inspection of the crystal structure, the DSG motif was found to make the closest contacts with mAb or β-TrCP.

The region after the DSGXXS motif is less important for binding. As evidenced by STD experiments, the C-terminal A39-G48 region of P-β-Cat$^{19–44}$ peptide is less implicated with mAb. In addition, the C-terminal region (starting from Ala39) appeared with less numerous NOEs constrains and a higher local rmsd. On the other hand, the NH of the Trp25 and His36 aromatic residues are recognized as evidenced by STD NMR experiments. Aromatic protons which classically possessed larger T_1 relaxation times relative to other protons found in peptides or proteins could be overestimated in STD experiments

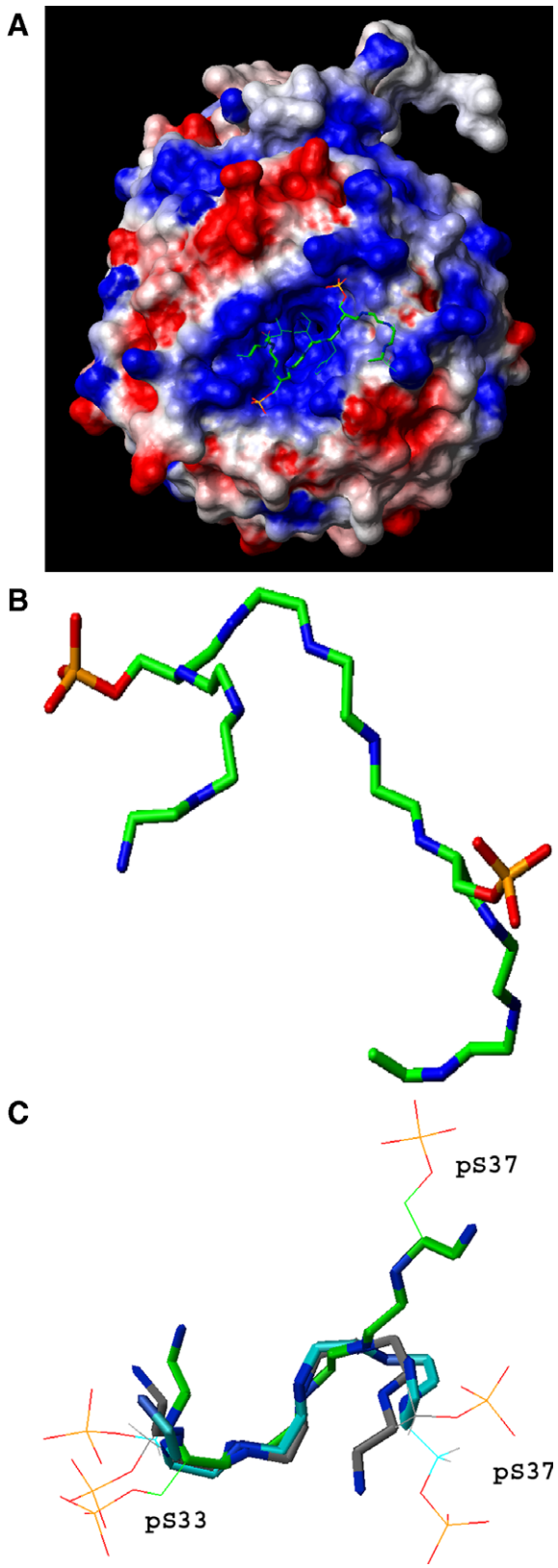

Fig. 9. (A) Surface representation of the top face of the β-TrCP WD40 domain with the bound D**pS**GXX**pS** motif from the crystal structure of the human β-TrCP-SkP1 complex bound to a β-Catenin substrate peptide [40]. The surface is colored according to the electrostatic potential (red for the negative region and blue for thee positive surface).

[41]. Even if the relaxation delay was increased up to seven times of T_1 (the average value for T_1 was around 500 ms), signals of Trp25 and essentially those coming from the aromatic chain were always the stronger ones observed in STD experiment. Tryptophan is a rarely found aromatic residue (1.2%) and its position upstream of the DSG motif could reflect the particular role of tryptophan as that had been observed in the study of the interaction of β-Catenin with β-TrCP [28]. His24 and Trp25 whose hydrophobic nature is conserved in the peptide fragment (in white, Fig. 7A) are able to make hydrophobic and/or π–π interactions with a hydrophobic pocket in mAb. The antibody was developed against a synthetic peptide (^{32}**DpS** GIH**pS**GATTTAPS^{45}), however the NMR studies performed with mAb and P-β-Cat$^{19–44}$ show that a region of sequence upstream of the DSG motif that was not included in the antigenic peptide directly contacts mAb. These contacts could be assigned as non-specific. However, residues His24 and Trp25 are in close proximity to the DSG motif and they could participate to increase indirectly the affinity of the binding region.

Finally, the NMR data described above show that the epitope comprises a surface extending over residues of the D**pS**GXX**pS**motif, with contributions being made by the main chain of hydrophobic residues His24 and Trp25. These observations are consistent with the sequence requirements playing a role in interaction with the β-TrCP protein, the bend D**pS**GXX**pS** motif of the bound P-β-Cat$^{19–44}$ peptide associated with the hydrophobic and/or π–π cluster (H24-W25).

The refined conformation of the P-β-Cat$^{19–44}$ peptide in the binding sites of its monoclonal antibody is necessary to understand the biological action of the overall β-Catenin protein phosphorylated at sites pSer33 and pSer37. The data presented here are important for refining the bound phosphorylated structures and provide valuable assistance in the interpretation of the NMR investigation of the complexes of these peptides linked to their binding proteins. Taken together, our data are consistent with the idea that the specific monoclonal antibody and β-TrCP interactions with the phosphorylated peptide are to a great extent analogous. The similarities observed in the P-β-Cat$^{17–48}$ peptide (including the phosphorylation motif DpS^{33}GXXpS^{37}) while bound to β-TrCP in conjunction with highly refined structures free in solution and in the antibody-bound states, will facilitate understanding of the basic mechanisms involved in β-TrCP-receptor interactions and proteasome targeting of the oncogenic protein β-Catenin.

4. Materials and methods

4.1. Peptides

β-Catenin (β-Cat) fragments (residues 19–44), the P-β-Cat$^{19–44}$ (and β-Cat$^{19–44}$) peptides containing phosphorylated sites 33 and 37 with the Ac-K^{19}AAVSHWQQQSYLD**pS**GIH**pS**GATTTAP^{44}-NH_2 amino acid sequence, were synthesized in the group of Francoise Baleux, Pasteur Institute (Paris, France). The purity of the peptides (90%) was tested by analytical HPLC and by mass spectrometry.

Fig. 9 (B) Close-up view of the D**pS**GXX**pS** motif, from the crystal structure and recognized by the F-box protein β-TrCP [40]. (C) Superimposition of the ^{32}D**pS**GXX**pS**^{37} fragment of the mAb P-β-Cat$^{19–44}$ bound peptide (in blue), the β-TrCP-P-β-Cat$^{17–48}$ bound peptide (in grey) [28] and the crystal structure (in green) [40].

4.2. Monoclonal antipeptide antibody BC-22

Monoclonal anti-diphospho P-β-Cat (pSer33 and pSer37) was purchased from Sigma–Aldrich (Ref. C4231, clone BC-22, referred to as mAb antibody). This antibody (mouse IgG2b isotype) was developed against a synthetic peptide (^{32}**DpS** GIH**pS**GATTTAPS^{45}) corresponding to amino acids 32–45 (pSer33 and pSer37) of Human β-Catenin conjugated to KLH (Keyhole Limpet Hemocyanin). Nonphosphorylated or monophosphorylated (Ser33) peptides were used as a negative control. The antibody concentration was estimated to be ~2 mg/mL with an approximate molecular mass of 160 kDa, in a solution 20 mM phosphate buffered saline (pH 7.4), containing 15 mM sodium azide. This amount of purified antibody was used to prepare the NMR samples.

4.3. NMR experiments

^{1}H NMR spectra were recorded at 278 K on a Bruker Avance-500 spectrometer using a *z*-axis gradient. Chemical shifts assignments (Tables 1 and 2) refer to internal 3-(trimethylsilyl)propionic acid-*2,2,3,3-d*$_4$ sodium salt (TSP-*d*$_4$). Two-dimensional NMR spectra were recorded in the phase-sensitive mode using the States-time-proportional phase incrementation method [42]. All experiments were carried out using the 3-9-19 binomial water suppression by gradient-tailored excitation pulse sequence for water suppression [43]. Two-dimensional ^{1}H–^{1}H TOCSY spectra were recorded using a MLEV-17 spin-lock sequence [44] with a mixing time of 70 ms. Typically, spectra were acquired with 256 t_1 increments, 2048 data points, and a relaxation delay of 1.5 s. Spectra were processed using XWIN NMR software. All spectra were zero-filled in the F_1 spectral dimension to 1024 data points followed by forward linear prediction of 512 points. Finally, a square cosine bell window function was applied in both dimensions prior to Fourier transformation. For preparation of NMR peptide-antibody samples, the antibody solution (200 μl) was diluted in NMR phosphate buffer (20 mM phosphate, 5% D_2O, and 0.02% NaN_3) at pH 7.2. The final sample (250 μl in a Shigemi tube) contained 0.4 mg of antibody (0.01 mM) and 1 mM peptide, leading to a ligand:antibody ratio of 100:1.

For STD experiments (Fig. 2), the one-dimensional (1D) ^{1}H STD NMR [31,32,45] spectra of the mAb-peptide complex (Fig. 2A) were recorded at 500 MHz with 2048 scans and selective saturation of protein resonances at 12 ppm or −3 ppm (30 ppm for reference spectra) showing that by irradiating at −3 ppm, the antibody can be saturated uniformly and can therefore be efficiently used for the STD NMR technique. Investigation of the time dependence of the saturation transfer with saturation times from 0.2 to 4.0 s showed that 2 s was needed for efficient transfer of saturation from the protein to the ligand protons. STD NMR spectra were acquired using a series of 40 equally spaced 50 ms Gaussian-shaped pulses for selective saturation (then, a total saturation time was of approximately 2 s) [46], with 1 ms delay between the pulses. With an attenuation of 50 dB, the radiofrequency field strength for the selective saturation pulses in all STD NMR experiments was 186 Hz. Subtraction of FID values with on- and off-resonance protein saturation was achieved by phase cycling.

Transferred nuclear Overhauser effect (TRNOESY) [36] spectra of the mAb-peptide complex were recorded with 4 K points and 512 t_1 increments, and a relaxation delay of 1 s. Data processing were performed by zero filling to 1 K points in F_1 to give a final 4 K × 1 K matrix. The bound and free states exist in the same regime, namely $\omega\tau_c > 1$; thus, the cross-relaxation rates of the P-β-Cat$^{19–44}$ peptide (MW = 2943 g/mol) in the free and bound state are negative in sign. The optimal conditions for the TRNOESY measurements were determined by considering a peptide:mAb molar ratio ranging from 100 to 200 with mixing times (τ_m) of 50, 100, 200, 400 and 600 ms. The build-up curve [37] for different NOE correlations showed that spin diffusion was negligible for a τ_m of 200 ms (Fig. 4). The faster rate of build-up for the pairs (intra-residue HN/Hα NOEs for His36 and pSer37) in the bound state vs the free state, as shown in Fig. 4, indicated that the effects are representative of the bound state. The observed TRNOE correlations with mixing times of 100 and 200 ms were intense and negative. They were assigned to the mAb-bound antigen [47] as a sample of the peptide without the presence of antibody exhibited only intra-residue and sequential NOE intensities with a mixing time of 200 ms. Automatic baseline correction was performed prior to integration of cross-peak volumes using FELIX (Accelrys). Cross-peaks intensities were converted to interproton distances using the distance between the two Tyr-aromatic protons (2.42 Å) as a reference. TRNOE cross-peaks classified as strong, medium, weak and very weak were converted into distance restraints of 1.8–2.7, 1.8–3.6, 1.8–5.0 and 1.8–6.0 Å, respectively.

4.4. Structure calculations

Distance restraints used in the structure calculations were derived from TRNOESY experiments performed with mixing time of 200 ms. The final list of distant restraints containing 311 unambiguous and 92 ambiguous restraints (194 intra-residue, 98 sequential, 98 medium-range and 13 long-range) (Table 3) was incorporated for structure calculation with the standard protocol of ARIA 1.2 [38,39]. Modifications of the phosphorylated residues (pSer) were introduced with CHARMM [48] for molecular dynamics calculations using the PARALLHDG 5.3 force field. During the calculations, non-glycine residues were restrained to negative ϕ values (usually the only range considered in NMR-derived structures) [49]. The simulated annealing protocol consisted of four stages: a high-temperature torsion angle simulated annealing phase at 10000 K (30 ps), a first torsion angle dynamics cooling phase from 10000 K to 50 K (15 ps), a second Cartesian dynamics cooling phase from 2000 K to 50 K (27 ps), and a final minimization phase at 50 K. ARIA enabled the incorporation of ambiguous distance restraints and calibration of the NOE restraints using automated matrix analysis as implemented by the program. ARIA runs were performed using the default parameters with eight iterations. Twenty structures were generated each round, and the 10 lowest-energy structures were carried on to the next iteration. In the final iteration, the 20 lowest-energy structures were retained as the final structures. Even if ARIA is able to generate structures of the free peptide with a final energy minimization step in a simulated water box, it was decided that due to the presence of the bound peptide in the hydrophobic antibody recognition sites this step was not applicable. The set of P-β-Cat$^{19–44}$ structures was selected for correct geometry and no distances restraint violations of >0.5 Å. Analysis of the structures was performed within Aqua, PROCHECK NMR [50] programs (Table 3). MOLMOL [51] was used for the analysis and presentation of the results of the structure determination.

5. Notes

The coordinates were deposited in the Protein data Bank with the following code: 2G57. The chemical shift assignment Tables were deposited in the Biomagnetic Resonance Data Bank with the BMRB accession number: 7001.

Acknowledgement: This work was supported by grants from the organisms Sidaction, ARC (Association pour la Recherche sur le Cancer) and FRM (Fondation pour la Recherche Médicale). Simon MEGY is supported by FRM.

Appendix A. Supplementary data

Figures TRNOESY spectrum of the P-β-Cat$^{19–44}$ peptide in the presence of the GST-β-TrCP protein, and a NOESY spectrum of P-β-Cat$^{19–44}$ peptide. Supplementary data associated with this article can be found, in the online version, at doi:10.1016/j.febslet.2006.08.084.

References

[1] Behrens, J., von Kries, J.P., Kuhl, M., Bruhn, L., Wedlich, D., Grosschedl, R. and Birchmeier, W. (1996) Functional interaction of beta-catenin with the transcription factor LEF-1. Nature 382, 638–642.

[2] Huber, O., Korn, R., McLaughlin, J., Ohsugi, M., Herrmann, B.G. and Kemler, R. (1996) Nuclear localization of beta-catenin by interaction with transcription factor LEF-1. Mech. Dev. 59, 3–10.

[3] Moon, R.T., Brown, J.D. and Torres, M. (1997) WNTs modulate cell fate and behavior during vertebrate development. Trends Genet. 13, 157–162.
[4] Cadigan, K.M. and Nusse, R. (1997) Wnt signaling: a common theme in animal development. Genes Dev. 11, 3286–3305.
[5] Peifer, M. (1997) Beta-catenin as oncogene: the smoking gun. Science 275, 1752–1753.
[6] Kinzler, K.W. and Vogelstein, B. (1996) Lessons from hereditary colorectal cancer. Cell 87, 159–170.
[7] Aberle, H., Bauer, A., Stapper, J., Kispert, A. and Kemler, R. (1997) Beta-catenin is a target for the ubiquitin-proteasome pathway. EMBO 16 (13), 3797–3804.
[8] Hattori, K., Hatakeyama, S., Shirane, M., Matsumoto, M. and Nakayama, K. (1999) Molecular dissection of the interactions among IkappaBalpha, FWD1, and Skp1 required for ubiquitin-mediated proteolysis of IkappaBalpha. J. Biol. Chem. 274, 29641–29647.
[9] Hershko, A. (1983) Ubiquitin: roles in protein modification and breakdown. Cell 34, 11–12.
[10] Kitagawa, M., Hatakeyama, S., Shirane, M., Matsumoto, M., Ishida, N., Hattori, K., Nakamichi, I., Kikuchi, A. and Nakayama, K. (1999) An F-box protein, FWD1, mediates ubiquitin-dependent proteolysis of beta-catenin. EMBO J. 18, 2401–2410.
[11] Yost, C., Torres, M., Miller, J.R., Huang, E., Kimelman, D. and Moon, R.T. (1996) The axis-inducing activity, stability, and subcellular distribution of beta-catenin is regulated in Xenopus embryos by glycogen synthase kinase 3. Genes Dev. 10, 1443–1454.
[12] Sakanaka, C., Weiss, J.B. and Williams, L.T. (1998) Bridging of beta-catenin and glycogen synthase kinase-3beta by axin and inhibition of beta-catenin-mediated transcription. Proc. Natl. Acad. Sci. USA 95, 3020–3023.
[13] Behrens, J., Jerchow, B.A., Wurtele, M., Grimm, J., Asbrand, C., Wirtz, R., Kuhl, M., Wedlich, D. and Birchmeier, W. (1998) Functional interaction of an axin homolog, conductin, with beta-catenin, APC, and GSK3beta. Science 280, 596–599.
[14] Liu, C., Kato, Y., Zhang, Z., Do, V.M., Yankner, B.A. and He, X. (1999) beta-Trcp couples beta-catenin phosphorylation-degradation and regulates *Xenopus axis* formation. Proc. Natl. Acad. Sci. USA 96, 6273–6278.
[15] Hart, M., Concordet, J.-P., Lassot, I., Albert, I., Del los Santos, R., Durand, H., Perret, C., Rubinfeld, B., Margottin, F., Benarous, R. and Polakis, P. (1999) The F-box protein beta-TrCP associates with phosphorylated beta-catenin and regulates its activity in the cell. Curr. Biol. 9, 207–210.
[16] Winston, J.T., Strack, P., Beer-Romero, P., Chu, C.Y., Elledge, S.J. and Harper, J.W. (1999) The SCF β-TrCP-ubiquitin ligase complex associates specifically with phosphorylated destruction motifs in IκBα and β-catenin and stimulates IκBα ubiquitination in vitro. Genes Dev. 13, 270–283.
[17] Margottin, F., Bour, S., Durand, H., Selig, L., Benichou, S., Richard, V., Thomas, D., Strebel, K. and Benarous, R. (1998) A novel human WD protein, h-betaTrCP, that interacts with HIV-1 Vpu connects CD4 to the ER degradation pathway through an F-box motif. Mol. Cell 1, 565–574.
[18] Strebel, K., Klimkait, T., Maldarelli, F. and Martin, M.A. (1989) Molecular and biochemical analyses of human immunodeficiency virus type 1 vpu protein. J. Virol. 63, 3784–3791.
[19] Yaron, A., Hatzubai, A., Davis, M., Lavon, I., Amit, S., Manning, A.M., Andersen, J.S., Mann, M., Mercurio, F. and Ben-Neriah, Y. (1998) Identification of the receptor component of the IkappaBalpha-ubiquitin ligase. Nature 396, 590–594.
[20] Kroll, M., Margottin, F., Kohl, A., Renard, P., Durand, H., Concordet, J.-P., Bachelerie, F., Arenzana-Seisdedos, F. and Benarous, R. (1999) Inducible degradation of IkappaBalpha by the proteasome requires interaction with the F-box protein h-betaTrCP. J. Biol. Chem. 274, 7941–7945.
[21] Lassot, I., Ségéral, E., Berlioz-Torrent, C., Durand, H., Groussin, L., Hai, T., Benarous, R. and Margottin-Goguet, F. (2001) ATF4 degradation relies on a phosphorylation-dependent interaction with the SCFβ-TrCP ubiquitin ligase. Mol. Cell. Biol. 21, 2192–2202.
[22] Besnard-Guerin, C., Belaidouni, N., Lassot, I., Segeral, E., Jobart, A., Marchal, C. and Benarous, R. (2004) HIV-1 Vpu sequesters beta-transducin repeat-containing protein (betaTrCP) in the cytoplasm and provokes the accumulation of beta-catenin and other SCFbetaTrCP substrates. J. Biol. Chem. 279, 788–795.
[23] Sadot, E., Conacci-Sorrell, M., Zhurinsky, J., Shnizer, D., Lando, Z., Zharhary, D., Kam, Z., Ben-Ze'ev, A. and Geiger, B. (2002) Regulation of S33/S37 phosphorylated beta-catenin in normal and transformed cells. J. Cell Sci. 115, 2771–2780.
[24] Megy, S., Bertho, G., Gharbi-Benarous, J., Baleux, F., Benarous, R. and Girault, J.P. (2005) Solution structure of a peptide derived from the oncogenic protein beta-Catenin in its phosphorylated and nonphosphorylated states. Peptides 26, 227–241.
[25] Taub, R., Gould, R.J., Garsky, V.M., Ciccarone, T.M., Hoxie, J., Friedman, P.A. and Shattil, S.J. (1989) A monoclonal antibody against the platelet fibronogen receptor contains a sequence that mimics a receptor recognition domain in fibrinogen. J. Biol. Chem. 264, 259–265.
[26] Taub, R. and Greene, M.I. (1992) Functional validation of ligand mimicry by anti-receptor antibodies: structural and therapeutic implications. Biochemistry 31, 7431–7435.
[27] Calvete, J.J., Schafer, W., Mann, K., Henschen, A. and Gonzalez-Rodriguez, J. (1992) Localization of the cross-linking sites of RGD and KQAGDV peptides to the isolated fibrinogen receptor, the human platelet integrin glycoprotein IIb/IIIa. Influence of peptide length. Eur. J. Biochem. 206, 759–765.
[28] Megy, S., Bertho, G., Gharbi-Benarous, J., Baleux, F., Benarous, R. and Girault, J.P. (2005) STD and TRNOESY NMR Studies on the conformation of the oncogenic protein b-Catenin containing the phosphorylated motif DpSGXXpS bound to the b-TrCP protein. J. Biol. Chem. 280, 29107–29116.
[29] Ni, F. (1994) Recent developments in transferred NOE methods. Progr. Nucl. Mag. Reson. Spectrosc. 26, 517–606.
[30] Klein, J., Meinecke, R., Mayer, M. and Meyer, B. (1999) Detecting binding affinity to immobilized receptor proteins in compound libraries by HR-MAS STD NMR. J. Am. Chem. Soc. 121, 5336–5337.
[31] Mayer, M. and Meyer, B. (1999) Characterization of ligand binding by saturation transfer difference NMR spectroscopy. Angew. Chem., Int. Ed. Engl. 38, 1784–1788.
[32] Mayer, M. and Meyer, B. (2001) Group epitope mapping by saturation transfer difference NMR to identify segments of a ligand in direct contact with a protein receptor. J. Am. Chem. Soc. 123, 6108–6117.
[33] Wüthrich, K. (1986)NMR of Proteins and Nucleic Acids, Wiley, New York.
[34] Johnson, M.A., Jaseja, M., Zou, W., Jennings, H.J., Copié, V., Pinto, B.M. and Pincus, S.H. (2003) NMR studies of carbohydrates and carbohydrate-mimetic peptides recognized by an Anti-Group B Streptococcus antibody. J. Biol. Chem. 278, 24740–24752.
[35] Kooistra, O., Herfurth, L., Luneberg, E., Frosch, M., Peters, T. and Zahringer, U. (2002) Epitope mapping of the O-chain polysaccharide of *Legionella pneumophila* serogroup 1 lipopolysaccharide by saturation-transfer-difference NMR spectroscopy. Eur. J. Biochem. 269, 573–582.
[36] Clore, G.M. and Gronenborn, A.M. (1983) Theory of the time dependent transferred nuclear Overhauser effect: applications to structural analysis of ligand-protein complexes in solution. J. Magn. Reson. 53, 423–442.
[37] Kumar, A., Wagner, G., Ernst, R.R. and Wüthrich, K. (1981) Buildup rates of the NOE measured by 2D Proton Magnetic Resonance Spectroscopy: Implication for studies of protein conformation. J. Am. Chem. Soc. 103, 3654–3658.
[38] Brünger, A.T., Adams, P.D., Clore, G.M., Gros, P., Grosse-Kunstleve, R.W., Jiang, J.S., Kuszewski, J., Nilges, M., Pannu, N.S., Read, R.J., Rice, L.M., Smonson, T. and Warren, G.L. (1998) Crystallography & NMR system (CNS): a new software system for macromolecular structure determination. Acta Cryst. D 54, 905–921.
[39] Linge, J.P., Habeck, M., Rieping, W. and Nilges, M. (2003) ARIA: automated assignment and NMR structure calculation. Bioinformatics 19, 315–316.
[40] Wu, G., Xu, G., Schulman, B.A., Jeffrey, P.D., Harper, J.W. and Pavletich, N.P. (2003) Structure of a beta-TrCP1-Skp1-beta-catenin complex: destruction motif binding and lysine specificity of the SCF(beta-TrCP1) ubiquitin ligase. Mol. Cell 11, 1445–1456.
[41] Yan, J., Kline, A.D., Mo, H., Shapiro, M.J. and Zartler, E.R. (2003) The effect of relaxation on the epitope mapping by

saturation transfer difference NMR. J. Magn. Reson. 163, 270–276.
[42] States, D.J., Haberkorn, R.A. and Ruben, D.J. (1982) A two-dimensional nuclear Overhauser experiment with pure absorption phase in four quadrants. J. Magn. Res. 48, 286–292.
[43] Piotto, M., Saudek, V. and Sklenar, V. (1992) Gradient-tailored exitation for single-quantum NMR spectroscopy of aqueous solutions. J. Biomol. NMR 2, 661–665.
[44] Bax, A. and Davis, D.G. (1985) MLEV-17-based two-dimensional homonuclear magnetization transfer spectroscopy. J. Magn. Reson. 65, 355–360.
[45] Klein, J., Meinecke, R., Mayer, M. and Meyer, B. (1999) Detecting binding affinity to immobilized receptor proteins in compound libraries by HR-MAS STD NMR. J. Am. Chem. Soc. 121, 5336–5337.
[46] Meyer, B. and Peters, T. (2003) NMR spectroscopy techniques for screening and identifying ligand binding to protein receptors. Angew. Chem., Int. Ed. Engl. 42, 864–890.
[47] Cung, M.T., Demange, P., Marraud, M., Tsikaris, V., Sakarellos, C., Papadouli, I., Kokla, A. and Tzartos, S.J. (1991) Two-dimensional 1H NMR study of antigene-antibody interactions : Binding of synthetic decapeptides to an anti-acetylcholine receptor monoclonal antibody. Biopolymers 31, 769–776.
[48] Brooks, B.R., Bruccoleri, R.E., Olafson, B.D., States, D.J., Swaminathan, S. and Karplus, M. (1983) CHARMM: a program for macromolecular energy, minimization, and dynamics calculations. J. Comput. Chem. 4, 187–217.
[49] Schibli, D.J., Montelaro, R.C. and Vogel, H.J. (2001) The membrane-proximal tryptophan-rich region of the HIV glycoprotein, gp41, forms a well-defined helix in dodecylphosphocholine micelles. Biochemistry 40, 9570–9578.
[50] Otting, G. (1993) Experimental NMR techniques for studies of protein-ligand interactions. Curr. Open. Struct. Biol. 3, 760–768.
[51] Koradi, R., Billeter, M. and Wüthrich, K. (1996) MOLMOL: a program for display and analysis of macromolecular structures. J. Mol. Graph. 14, 51–55, 29–32.
[52] Huber, A.H., Nelson, W.J. and Weis, W.I. (1997) Three-dimensional structure of the armadillo repeat region of beta-catenin. Cell 90, 871–882.